

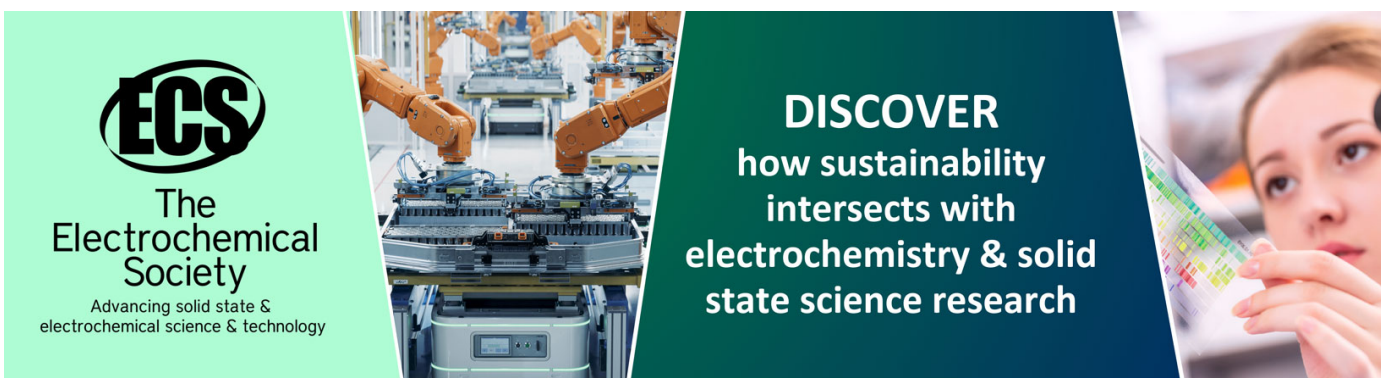
## Low energy dissipation electric circuit for energy harvesting

To cite this article: Kanjuro Makihara *et al* 2006 *Smart Mater. Struct.* **15** 1493

View the [article online](#) for updates and enhancements.

### You may also like

- [A comparative analysis of parallel SSHI and SEH for bistable vibration energy harvesters](#)  
Quentin Demouron, Adrien Morel, David Gibus *et al.*
- [Multimodal piezoelectric energy harvesting on a thin plate integrated with SSHI circuit: an analytical and experimental study](#)  
Seyed Morteza Hoseyni, Mehmet Simsek, Amirreza Aghakhani *et al.*
- [Numerical modeling and analysis of self-powered synchronous switching circuit for the study of transient charging behavior of a vibration energy harvester](#)  
Shahriar Bagheri, Nan Wu and Shaahin Filizadeh



**ECS**  
The  
Electrochemical  
Society  
Advancing solid state &  
electrochemical science & technology

**DISCOVER**  
how sustainability  
intersects with  
electrochemistry & solid  
state science research

# Low energy dissipation electric circuit for energy harvesting

Kanjuro Makihara<sup>1</sup>, Junjiro Onoda<sup>1</sup> and Takeya Miyakawa<sup>2</sup>

<sup>1</sup> Institute of Space and Astronautical Science, Japan Aerospace Exploration Agency, 3-1-1 Yoshinodai, Sagami-hara, Kanagawa 229-8510, Japan

<sup>2</sup> The University of Tokyo, Tokyo 113-8656, Japan

E-mail: [kanjuro@svs.eng.isas.jaxa.jp](mailto:kanjuro@svs.eng.isas.jaxa.jp) and [onoda@isas.jaxa.jp](mailto:onoda@isas.jaxa.jp)

Received 28 March 2006, in final form 13 July 2006

Published 15 September 2006

Online at [stacks.iop.org/SMS/15/1493](http://stacks.iop.org/SMS/15/1493)

## Abstract

A low energy dissipation circuit is proposed to achieve more effective energy harvesting, called ‘synchronized switch harvesting on inductor (SSHI)’. The proposed circuit only has two diodes, while the original SSHI circuit has four diodes comprising a diode bridge. It thus reduces the voltage drop during the energy-harvesting process, because the actual diodes have forward voltage regarded as equivalent electrical resistance or energy dissipation.

Energy-harvesting experiments demonstrated that the proposed circuit increases the harvested energy output to as much as 120% of that for the original SSHI circuit. We confirmed that the storage voltage in the steady state is independent of the storage capacitance through extensive energy-harvesting experiments, and that the settling time of the storage voltage is proportional to the storage capacitance but independent of the harvesting circuit.

## 1. Introduction

Energy harvesting is the process by which energy is captured and stored. There is a variety of different methods for harvesting energy, such as solar power, ocean tides, piezoelectricity, thermoelectricity, and physical motion. Energy-harvesting techniques will be vital in the future, as fossil fuels run out. From these various possibilities, this paper focuses on energy harvesting from vibrating structures using piezoelectricity. The piezoelectric energy-harvesting technique has been investigated intensively, as reviewed by Sodano *et al* [1]. Ottman *et al* [2, 3] worked on research of an adaptive DC–DC converter to maximize the power output from piezoelectric materials. Lesieutre *et al* [4] addressed the damping associated with harvesting electrical energy from a mechanically excited piezoelectric structure. Cornwell *et al* [5] proposed an approach for improving power output by using a tuned auxiliary structure. Kim *et al* [6] discussed structural factors to maximize electrical energy output in relation to given constraints.

A promising method of energy harvesting called ‘synchronized switch harvesting on inductor (SSHI)’ was recently proposed by Badel *et al* [7]. This and other related techniques [8, 9] use an electric circuit composed of a

piezoelectric transducer, an inductor, an on–off switch, and a diode bridge. SSHI is based on a preceding method of vibration suppression that is called ‘synchronized switching damping on inductor (SSDI)’. The original SSDI uses a piezoelectric transducer connected to an inductive circuit having an on–off switch. It reverses the polarity of the transducer’s voltage to effectively suppress vibration by exploiting the first half period of electrical vibration in the inductive circuit. The original SSDI and other relevant vibration suppression methods have been proposed by a few research groups [10–13]. Mechanical energy is converted to electrical energy through the piezoelectric transducer, and the converted electrical energy is reused to suppress structural vibrations, instead of simply being dissipated. Energy loss would crucially deteriorate a system’s performance in both SSDI and SSHI systems, and a great deal of attention has thus far been paid to preventing the energy loss caused by electrical resistors. To improve energy harvesting with SSHI, it is imperative to keep the resistance value of the circuit as low as possible.

## 2. SDOF system with piezoelectric transducer

This paper features a piezoelectric transducer to convert mechanical vibration energy to electrical energy. As is

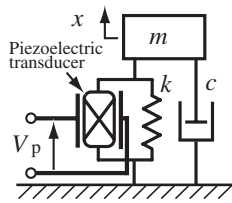


**Figure 1.** SDOF system attached to a single piezoelectric transducer.

well known, a piezoelectric transducer exerts force that is proportional to the applied voltage [14]. The relationship between the tensile force  $f$ , elongation  $x$ , and voltage  $V_p$  can thus be expressed as

$$f = k_p x - b_p V_p, \tag{1}$$

where  $k_p$  is the constant-voltage stiffness and  $b_p$  is the piezoelectric constant. A piezoelectric transducer can be electrically modeled as a combination of a voltage generator and a capacitor. The voltage generator represents the piezoelectric effect caused by structural motion.  $C_p$  is the constant-elongation capacitance of the piezoelectric transducer.

To simplify the energy-harvesting analysis, let us consider a single degree-of-freedom (SDOF) system that has one vibration mode. The SDOF system with a piezoelectric transducer (figure 1) is assumed to have a mass of  $m$ , a damping element of  $c$ , and a total stiffness of  $k$  including  $k_p$ . The equation of motion for the system is written as

$$m\ddot{x} + c\dot{x} + kx = b_p V_p, \tag{2}$$

where  $x$  is the displacement of the mass. From a fundamental analysis of controlling vibration, if the polarity of  $V_p$  is equal to that of  $-\dot{x}$ ,  $b_p V_p$  in equation (2) can be regarded as an additional damping element that deprives the system of vibration energy. Therefore, we can obtain one vibration-control logic; when  $\dot{x}$  is positive,  $V_p$  should be negative, and when  $\dot{x}$  is negative,  $V_p$  should be positive. SSDI is one method of implementing this vibration-control logic in the piezoelectric system, which utilizes an inductive circuit having an on-off switch. According to previous studies, when the vibration displacement of the SDOF system reaches a peak (i.e., the velocity is zero), the on-off switch is on for the half period of the electrical vibration to reverse the piezoelectric voltage polarity. The electrical vibration is caused by the combination of inductance  $L$  of the circuit and capacitance  $C_p$  of the piezoelectric transducer. The half period of the electrical vibration  $\tau$  is almost  $\pi\sqrt{LC_p}$  as long as the circuit resistance is quite small.

### 3. Original circuit for SSHI

We will now explain SSHI and its electric circuit to enable a better understanding compared to the idea we propose. Figure 2 is a schematic illustration of the original SSHI circuit. The diode bridge is a full-wave bridge rectifier utilizing four diodes in a bridge configuration to convert alternating current (AC) into direct current (DC). The capacitor,  $C_s$ , stores the electrical energy obtained by the energy-harvesting process.

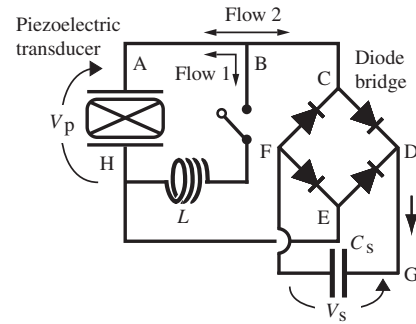


**Figure 2.** Original circuit for SSHI.

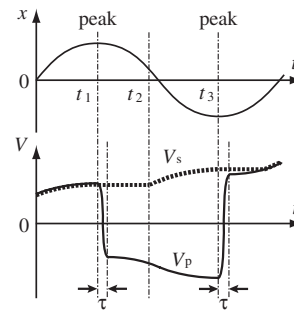


**Figure 3.** Schematic illustration of SSHI mechanism.

The storage capacitor is an element of electrical loads, namely a supplied target of the energy-harvesting system. It can thus be substituted with other electrical elements, such as resistors and DC-DC converters.

As described earlier, when the vibration displacement reaches a peak (minimum or maximum), the on-off switch is on for the duration of  $\tau$ . When the on-off switch is on, electric current flows in a branch circuit (represented by points A, B, L, and H in figure 2). This figure refers to this electric current as flow 1.

On the one hand, when  $V_p$  is positive at a displacement peak (e.g.,  $t = t_1$  in figure 3), electric current flows clockwise (A → B → L → H) after the switch is on. This inductive circuit requires a duration of  $\tau$  to reverse the polarity of  $V_p$  and to reach the next minimum of  $V_p$ . The current flow in this branch circuit completes within the duration of  $\tau$ , which is usually very short compared to the period of mechanical vibration. On the other hand, when  $V_p$  is negative at a displacement peak (e.g.,  $t = t_3$  in figure 3), electric current flows in the opposite direction (H → L → B → A) after the switch is on. In brief, the electric flow in this branch circuit (flow 1) has a ‘voltage-reverse mechanism’ for reversing the polarity of  $V_p$  with the help of electrical vibration. This mechanism originates from the preceding SSDI.

The original circuit (figure 2) has another branch circuit (represented by points A, B, C, D, E, F, G, and H). While the absolute value of  $V_p$  is smaller than  $V_s$ , no electric current flows in this branch circuit. During this time, the absolute value of  $V_p$  increases according to structural motion due to the piezoelectric effect. When the absolute value of  $V_p$  reaches  $V_s$  (e.g.,  $t = t_2$  in figure 3), electric current starts to flow in this

circuit branch. Figure 2 refers to this flow as flow 2. When  $V_p (>0)$  is larger than  $V_s$ , current flows along one circular route ( $A \rightarrow B \rightarrow C \rightarrow D \rightarrow G \rightarrow F \rightarrow E \rightarrow H$ ). Contrarily, when  $V_p (<0)$  is smaller than  $-V_s$ , current flows along another circular route ( $H \rightarrow E \rightarrow D \rightarrow G \rightarrow F \rightarrow C \rightarrow B \rightarrow A$ ). In both routes for flow 2, the piezoelectric transducer's electrical energy is transferred to the capacitor,  $C_s$ , to be stored. As can be seen from figure 3, this process of transferring energy continues as long as  $V_s$  is smaller than the absolute value of  $V_p$ . Electric flow 2 has an 'energy-harvesting mechanism' assisted by the diode bridge, which is the standard AC-DC conversion technique.

In summary, SSHI has a 'voltage-reverse mechanism' and an 'energy-harvesting mechanism'. SSHI needs two respective branch circuits to achieve the two mechanisms and the corresponding electrical flows (flows 1 and 2).

It needs to be emphasized that the aforementioned analysis is based on the use of ideal electrical equipment with no energy dissipation. However, as will be explained in the next section, the actual original circuit (figure 2) has energy dissipation resulting from diodes in the diode bridge, as well as wire resistance and equivalent resistance of the piezoelectric transducer [15]. To be more specific, the original circuit suffers from the energy dissipation that is caused by two diodes. This is because the electric flow for energy harvesting (flow 2) always goes through two diodes. The energy dissipation resulting from the diodes may deteriorate a system's energy-harvesting efficiency.

#### 4. Energy dissipation by actual diodes

This paper focuses on the energy dissipation of an actual diode. Generally speaking, a diode allows electric current to flow in one positive direction, but essentially blocks it in the opposite direction. However, even if positive voltage is applied to the diode in the positive direction, while the applied voltage is small, electric current does not flow through the diode. Only when the applied voltage is greater than a threshold, which is often called 'forward voltage', does electric current flow through the diode [16]. Any of the commercially available diodes has a forward voltage of at least 0.6 V. There is an active emulating diode that is composed of an operational amplifier and a voltage source, which provides a smaller value of equivalent resistance. But such an active emulating component requires some electrical energy for operation. The use of such an active electrical device has not been adopted in this paper, with its single objective of energy harvesting.

The forward voltage of an actual diode can be regarded as equivalent electrical resistance or energy dissipation, since it dissipates the electrical energy of the electric current flowing through the diode. From the energy-harvesting viewpoint, the dissipation of energy in diodes should be reduced as much as possible. We thus have searched for a new energy-harvesting circuit that would reduce the energy dissipation or the number of diodes.

#### 5. Proposed circuit for low energy dissipation

We propose a novel circuit (figure 4) that only has two diodes and a selector switch, in contrast to the original SSHI

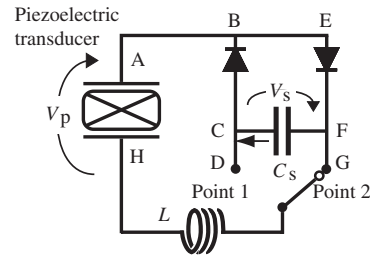


Figure 4. New circuit for SSHI.

circuit (figure 2) with four diodes comprising a diode bridge. This selector switch is connected to point 1 or 2 to control current flow, instead of the short time an on-off switch is on. The substitution of a selector switch with an on-off switch was originally proposed for the purpose of vibration suppression [13] and a comprehensive comparison of switch properties has already been discussed [17]. This paper further develops this idea of the selector switch, and describes the advantages of the circuit we propose over the original SSHI circuit. When it comes to SDOF systems, similar to the original SSHI circuit, the circuit we propose changes the switch connection depending on the velocity of the mechanical vibration. More specifically, when the velocity is negative, the switch connects point 2, whereas when the velocity is positive, the switch connects point 1.

On the one hand, when the displacement reaches a peak and when  $V_p$  is positive (e.g.,  $t = t_1$  in figure 3),  $V_p$  is expected to change its polarity from positive to negative. When the selector switch is connected to point 2 from point 1, electric current starts to flow along one circular route ( $A \rightarrow B \rightarrow E \rightarrow F \rightarrow G \rightarrow L \rightarrow H$ ). Due to this current flow, the polarity of  $V_p$  is reversed to negative. After  $V_p$  reaches the minimum peak, the diode between points E and F prevents electric current from flowing in the opposite direction, and  $V_p$  retains the minimum negative value. This current flow is responsible for the 'voltage reverse mechanism'. After this voltage-reverse mechanism has been completed, while  $-V_p$  is smaller than  $V_s$ , no electric current flows in any branch circuit. During this time,  $V_p$  decreases according to structural motion because of the piezoelectric effect. As soon as  $-V_p$  reaches  $V_s$  (e.g.,  $t = t_2$  in figure 3), electric current starts to flow along one circular route ( $H \rightarrow L \rightarrow G \rightarrow F \rightarrow C \rightarrow B \rightarrow A$ ), and some electric charge is stored in the capacitor. This current flow is responsible for the 'energy-harvesting mechanism'.

On the other hand, when the displacement reaches a peak and when  $V_p$  is negative (e.g.,  $t = t_3$  in figure 3),  $V_p$  is expected to change its polarity from negative to positive. When the selector switch is connected to point 1 from point 2, electric current flows along one circular route ( $H \rightarrow L \rightarrow D \rightarrow C \rightarrow B \rightarrow A$ ). Due to this current flow during  $\tau$ ,  $V_p$  will be positive. After that, when  $V_p$  reaches  $V_s$ , electric current starts to flow in one circular route ( $A \rightarrow B \rightarrow E \rightarrow F \rightarrow C \rightarrow D \rightarrow L \rightarrow H$ ), and some electric charge is stored in the capacitor.

Briefly, once the selector switch changes its connection point, the circuit we propose automatically achieves the voltage-reverse and energy-harvesting mechanisms. It should again be noted that the proposed circuit only has two diodes,

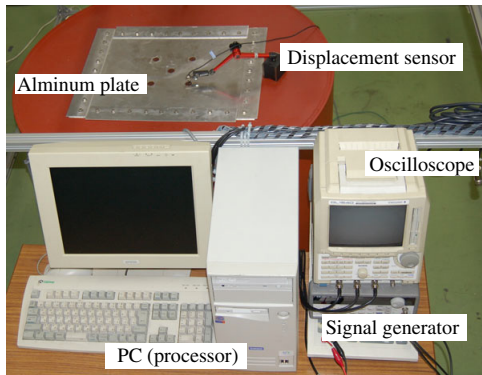


**Figure 5.** Photograph of experimental setup for energy harvesting. (This figure is in colour only in the electronic version)

instead of four. Electric current flows through only one diode along each energy-harvesting route, every time the piezoelectric transducer's electrical energy is transferred to the storage capacitor. Therefore, the new circuit is expected to have a smaller total resistance, and have a smaller amount of dissipated energy. This low energy dissipation circuit is preferable to the original, for application to energy-harvesting systems.

## 6. Experimental setup for energy harvesting

Only when its effectiveness has been proven in actual systems, can the proposed energy-harvesting circuit be utilized in real systems. We therefore carried out energy-harvesting experiments (figure 5). The aluminum plate (AL-5052) had an area of 0.45 m by 0.35 m and a thickness of 1.0 mm. The plate was rigidly supported on four boundaries. Commercially available piezoelectric transducers (Pb(ZrTi)O<sub>3</sub> ceramic C-91H, Fuji Ceramics Co., 60 mm × 40 mm × 0.5 mm) were employed for the energy-harvesting system. Eight sheets of the piezoelectric transducers were bonded on the plate surface. Each of four piezoelectric sheets was integrated into a group, and was electrically connected in parallel, as seen in figure 6. The two piezoelectric groups were placed in a centrosymmetric array about the plate center, and were electrically connected in parallel. Piezoelectric transducers have equivalent resistance that decreases with an increase in the number of cycles of input sinusoidal voltage [15]. Measuring actual transducers based on the research determined the equivalent resistance as 3.7 Ω. The first mode frequencies for an open circuit (i.e., constant charge) and for a shunt circuit (i.e., constant voltage) were 79.5 and 78.8 Hz, respectively, for the plate attached to the eight piezoelectric sheets. After iteration, the inductance was determined to be  $1.0 \times 10^{-2}$  H, which provided the most efficient harvesting. A commercially available inductor (100 mH High-power Choke-coil, ELC18B103L, Matsushita Electric Industrial Co.) was used. A commercially available diode bridge (Miniature Glass Passivated Single-phase Bridge Rectifier, DF005M, General Semiconductor Inc.) was employed for the original SSHI circuit. This diode bridge was composed of four diodes. To enable a fair comparison, two diodes out of these four were used to construct the proposed energy-harvesting circuit.

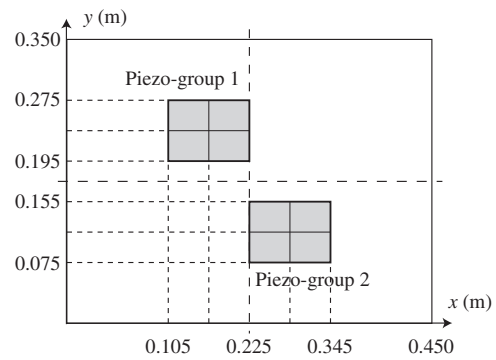


**Figure 6.** Piezoelectric sheets bonded on aluminum plate.

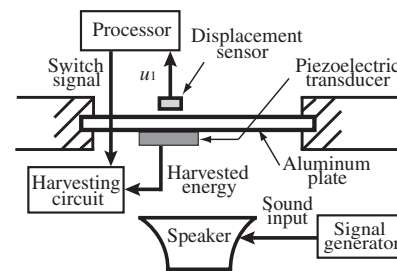


**Figure 7.** Experimental setup for the energy-harvesting system.

One displacement sensor was installed at the center of piezoelectric group 1 (i.e.,  $x = 0.165$  m and  $y = 0.235$  m in figure 6). The control flow in the experiment is outlined in figure 7. First, the measured displacement  $u_1$  was sent to a processor. Next, the processor calculated  $\dot{u}_1$  and, if necessary, sent a switch signal to the harvesting circuit. On receiving the signal, the circuit switch changed its connection status.

The aluminum plate's vibration was excited by the sound pressure generated from a speaker, and the sound pressure was applied uniformly over the plate area in the out-of-plane direction. The sound pressure had a sinusoidal force with the same frequency as the plate's first vibration mode.

## 7. Time histories for the energy-harvesting experiment

We first carried out an energy-harvesting experiment using the original SSHI circuit (figure 2) with a 10 μF storage capacitor. Figure 8 plots the time histories of the piezoelectric voltage and the storage voltage in the energy-harvesting experiment. At  $t = 0$  s, the aluminum plate started to vibrate with acoustic excitation. Energy-harvesting control was also commenced at the same time. As vibration excitation continued, the amplitude of structural vibration increased, and the amplitude of piezoelectric voltage also increased. Around  $t = 0.25$  s, the energy-harvesting system reached a steady state, where the amplitudes of the piezoelectric voltage and the storage voltage had converged. The converged value of the piezoelectric voltage was 7.5 V, and that of the storage voltage was 6.3 V. Figure 8 also compares the two voltages for a zoomed scale. The difference in the two voltages was 1.2 V. From the analytical prediction in the previous sections, this voltage

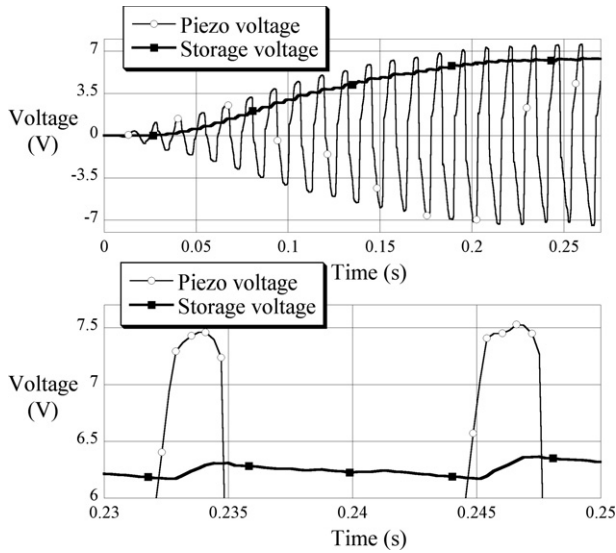


Figure 8. Experimental results using the original circuit (figure 2).

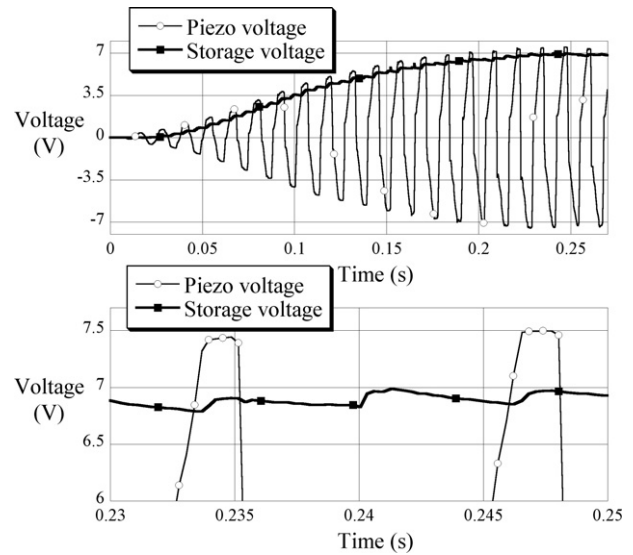


Figure 9. Experimental results using the proposed circuit (figure 4).

difference resulted from the two diodes in the diode bridge. This 1.2 V drop led to energy dissipation in the original SSHI system, and limited the energy-harvesting efficiency.

For comparison, we also carried out an energy-harvesting experiment with the proposed circuit (figure 4). This experiment also used the same  $10 \mu\text{F}$  storage capacitor as in the previous experiment. Figure 9 plots the time histories of the two voltages in the energy-harvesting experiment. The converged value of the piezoelectric voltage was 7.5 V, which was the same as in the previous experiment. However, the converged value of the storage voltage was 6.9 V. The difference in the two voltages was 0.6 V, while this was 1.2 V with the original SSHI circuit. This 0.6 V difference in the proposed circuit resulted from the one diode through which electric current flowed. This smaller voltage drop led to less dissipated energy in the energy-harvesting system. The proposed circuit increased the harvesting energy output to 120% of that for the original circuit (from  $1.98 \times 10^{-4}$  to  $2.38 \times 10^{-4}$  J). This increased harvesting energy is quite significant in actual harvesting systems. Considering the voltage drops in the two experiments, it turns out that diodes accounted for the majority of dissipated energy in this harvesting system. Through the harvesting experiments, we confirmed the benefits of reducing the number of diodes to improve the energy-harvesting efficiency.

We can see a gentle decrease of the storage voltage in these figures (e.g., between  $t = 0.235$  and  $0.240$  s in figure 9). This decrement was caused by energy dissipation in several monitoring devices, such as oscilloscopes and analog-digital converters. This dissipated energy should be reduced as much as possible in real harvesting systems.

## 8. Parametric studies on the energy-harvesting experiment

We did parametric studies on the energy-harvesting experiments by using four storage capacitors (10, 47, 100, and  $200 \mu\text{F}$ ).

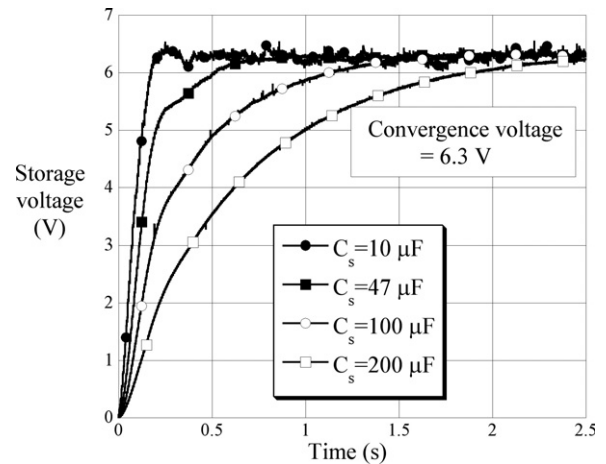
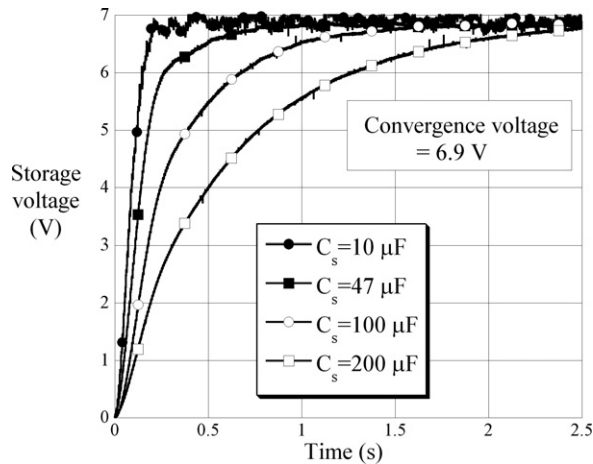


Figure 10. Time histories for energy harvesting using the original circuit (figure 2).

We first applied the original circuit (figure 2) to the energy-harvesting experiment. Figure 10 compares the time histories of the storage voltage in four cases of capacitance. All had a converged storage voltage of 6.3 V, and this was shown to be independent of capacitance,  $C_s$ . The settling time,  $t_s$ , of the storage voltage was defined as the duration needed for the voltage to converge. The settling times of the four systems were 0.25 s ( $C_s = 10 \mu\text{F}$ ), 0.75 s ( $C_s = 47 \mu\text{F}$ ), 1.5 s ( $C_s = 100 \mu\text{F}$ ), and 3.0 s ( $C_s = 200 \mu\text{F}$ ). The values of  $C_s/t_s$  were almost constant except for  $10 \mu\text{F}$ . Roughly speaking,  $(1/2) C_s V_{\text{convergence}}^2 / t_s$  represents the average work rate for the energy-harvesting systems. Because this average work rate is related to a system's inherent energy-harvesting capabilities, it is reasonable for  $C_s/t_s$  to be almost constant for one energy-harvesting system.

To compare performance, we also applied the proposed circuit (figure 4) to the energy-harvesting experiment. Figure 11 compares the time histories of the storage voltage in four cases of capacitance. All had a converged storage



**Figure 11.** Time histories for energy harvesting using the proposed circuit (figure 4).

voltage of 6.9 V. Similar to the earlier system, the converged voltage was independent of storage capacitance, as can be seen from figure 11. All settling times of the storage voltage were the same as the corresponding times in the original circuit system. Irrespective of storage capacitance, all harvested energy outputs of the proposed circuit increased to 120% of those in the original circuit.

## 9. Conclusions

We have proposed a low energy dissipation circuit that only has two diodes and a selector switch for more effective energy harvesting. This proposed circuit drastically decreases the voltage drop during the energy-harvesting process, because it reduces the number of diodes from those in the original 'synchronized switch harvesting on inductor (SSHI)' circuit. This is because the actual diodes have a forward voltage that can be regarded as equivalent resistance or energy dissipation. Once the selector switch changes its connection point, the system we propose automatically achieves the voltage-reverse and the energy-harvesting mechanisms.

Energy-harvesting experiments demonstrated that the circuit we propose sharply decreased the voltage drop from that in the original SSHI circuit. The harvested energy output increased to as much as 120%, when the same amplitude of piezoelectric voltage caused by structural vibration was applied. The storage voltage in the steady state was independent of storage capacitance. The settling time of the storage voltage was proportional to the storage capacitance but independent of the harvesting circuit configuration.

We evaluated the new circuit's advantages in the SSHI technique. However, this circuit's configuration, comprising two diodes and a selector switch, can, in principle, be applied to other piezoelectric energy-harvesting systems as long as a system is comprised of a switch element and a diode bridge, e.g., synchronous electric charge extraction [18]. Attempts to

reduce the number of diodes pave the way for a new circuit design in electrical energy transferring techniques.

## References

- [1] Sodano H A, Park G and Inman D J 2003 A review of power harvesting using piezoelectric materials *Shock Vib. Dig.* **36** 197–206
- [2] Ottman G K, Hofmann H F, Bhatt A C and Lesieutre G A 2002 Adaptive piezoelectric energy harvesting circuit for wireless remote power supply *IEEE Trans. Power Electron.* **17** 669–76
- [3] Ottman G K, Hofmann H K, Bhatt A C and Lesieutre G A 2003 Optimized piezoelectric energy harvesting circuit using stepdown converter in discontinuous conduction mode *IEEE Trans. Power Electron.* **18** 696–703
- [4] Lesieutre G A, Ottman G K and Hofmann H F 2003 Damping as a result of piezoelectric energy harvesting *J. Sound Vib.* **269** 991–1002
- [5] Cornwell P J, Goethal J, Kowko J and Daminakis M 2005 Enhancing power harvesting using a tuned auxiliary structure *J. Intell. Mater. Syst. Struct.* **16** 825–34
- [6] Kim S, Clark W W and Wang Q 2005 Piezoelectric energy harvesting with a clamped circular plate: analysis *J. Intell. Mater. Syst. Struct.* **16** 847–54
- [7] Badel A, Guyomar D, Lefeuvre E and Richard C 2005 Efficiency enhancement of a piezoelectric energy harvesting device in pulsed operation by synchronous charge inversion *J. Intell. Mater. Syst. Struct.* **16** 889–901
- [8] Guyomar D, Magnet C, Lefeuvre E and Richard C 2006 Power capability enhancement of a piezoelectric transformer *Smart Mater. Struct.* **15** 571–80
- [9] Guyomar D, Badel A, Lefeuvre E and Richard C 2005 Towards energy harvesting using active materials and conversion improvement by nonlinear processing *IEEE Trans. Ultrason. Ferroelectr. Freq. Control* **52** 584–95
- [10] Richard C, Guyomar D, Audigier D and Bassaler H 2000 Enhanced semi passive damping using continuous switching of a piezoelectric device on an inductor *Proc. SPIE Conf. on Damping and Isolation (Newport Beach)* vol 3989 (Bellingham, WA: SPIE Optical Engineering Press) pp 288–99
- [11] Corr L R and Clark W W 2002 Comparison of low-frequency piezoelectric switching shunt techniques for structural damping *Smart Mater. Struct.* **11** 370–6
- [12] Corr L R and Clark W W 2003 A novel semi-active multi-modal vibration control law for a piezoceramic actuator *ASME J. Vib. Acoust.* **125** 214–22
- [13] Onoda J, Makihara K and Minesugi K 2003 Energy-recycling semi-active method for vibration suppression with piezoelectric transducers *AIAA J.* **41** 711–9
- [14] Jaffe B, Cook W R Jr and Jaffe H 1971 *Piezoelectric Ceramics* (London: Academic)
- [15] Makihara K, Onoda J and Minesugi K 2006 Behavior of piezoelectric transducer on energy-recycling semi-active vibration suppression *AIAA J.* **44** 411–3
- [16] Fontaine G 1963 *Diodes and Transistors: General Principles* (Eindhoven: Philips Technical Library)
- [17] Makihara K, Onoda J and Minesugi K 2006 Comprehensive assessment of semi-active vibration suppression including energy analysis *ASME J. Vib. Acoust.* at press
- [18] Lefeuvre E, Badel A, Richard C and Guyomar D 2005 Piezoelectric energy harvesting device optimization by synchronous electric charge extraction *J. Intell. Mater. Syst. Struct.* **16** 865–76